Original Article

Preoperative evaluation of liver regeneration following hepatectomy in hepatocellular carcinoma using magnetic resonance elastography

Tong Zhang[1], Qian Li[1], Yi Wei[1], Shan Yao[1], Yuan Yuan[1], Liping Deng[1], Dongbo Wu[2], Lisha Nie[3], Xiaocheng Wei[3], Hehan Tang[1]^, Bin Song[1,4]^

[1]Department of Radiology, West China Hospital, Sichuan University, Chengdu, China; [2]Center of Infectious Diseases, West China Hospital, Sichuan University, Chengdu, China; [3]GE Healthcare China, Beijing, China; [4]Department of Radiology, Sanya People's Hospital, Sanya, China

Contributions: (I) Conception and design: T Zhang, Q Li, Y Wei, H Tang, B Song; (II) Administrative support: All authors; (III) Provision of study materials or patients: S Yao, Y Yuan, L Deng, H Tang; (IV) Collection and assembly of data: All authors; (V) Data analysis and interpretation: T Zhang, Q Li; (VI) Manuscript writing: All authors; (VII) Final approval of manuscript: All authors.

Correspondence to: Bin Song. Department of Radiology, West China Hospital, Sichuan University, 37 Guoxue Alley, Chengdu 610041, China; Department of Radiology, Sanya People's Hospital, 558 Jiefang Road, Sanya 572000, China. Email: songlab_radiology@163.com; Hehan Tang. Department of Radiology, West China Hospital, Sichuan University, 37 Guoxue Alley, Chengdu 610041, China. Email: 13980887312@163.com.

Background: For patients with hepatocellular carcinoma (HCC) undergoing hepatectomy, insufficient remnant liver regenerative capacity can lead to liver failure. The aim of this study was to evaluate the potential role of magnetic resonance elastography (MRE) for the preoperative prediction of liver regeneration in patients with HCC after partial hepatectomy (PH).

Methods: A total of 54 patients with HCC undergoing MRE prior to PH were retrospectively included. The total functional liver, volume of preoperative future liver remnant (LVpre), and volume of postoperative liver remnant (LVpost), respectively, were measured, and the regeneration index (RI) and parenchymal hepatic resection rate (PHRR) were manually calculated. Univariate and multivariate logistic regression analyses were conducted to identify factors associated with a high RI, and receiver operating characteristic (ROC) curves were employed to evaluate the diagnostic performance of the liver stiffness (LS) values. Patients were classified into three subgroups based on the value of PHRR: low PHRR (<30%), intermediate PHRR (30–50%), and high PHRR (>50%). Subsequently, Spearman correlation analysis was used to investigate the relationship between LS values and RI in the subgroups.

Results: Multivariable analysis revealed a low LS value was associated with greater odds of a high RI [odds ratio (OR), 0.049; 95% confidence interval (CI): 0.002 to 0.980]. An optimal cutoff value of 3.30 kPa was used to divide all patients into a low RI group and a high RI group with an area under the curve (AUC) value of 0.882 (95% CI: 0.767 to 0.996). A significant negative relationship between RI and LS values (r=–0.799; P<0.001) was observed in the intermediate PHRR subgroup.

Conclusions: The LS values based on MRE may serve as a potential preoperative predictor of liver regeneration for patients with HCC undergoing PH.

Keywords: Liver regeneration; elasticity imaging techniques; hepatocellular carcinoma (HCC); hepatectomy

Submitted Apr 01, 2022. Accepted for publication Aug 29, 2022.
doi: 10.21037/qims-22-306
View this article at: https://dx.doi.org/10.21037/qims-22-306

^ ORCID: Bin Song, 0000-0002-7269-2101; Hehan Tang, 0000-0002-3882-4270.

Introduction

Hepatocellular carcinoma (HCC) is the sixth most common malignancy and the fourth leading cause of cancer-associated mortality worldwide (1). Current treatments available for HCC include hepatectomy, radiofrequency ablation, liver transplantation, transarterial chemoembolization (TACE), and systemic chemotherapy (2,3), among which, surgical resection is considered the curative treatment (4,5). Although the liver can regenerate after hepatectomy, the regeneration is limited by various factors such as portal pressure and vascular outflow (6,7), and limited liver regeneration will result in an insufficient future remnant liver volume to support postoperative liver function, eventually leading to liver failure (8-10). Consequently, accurate preoperative prediction of the ability of remnant liver to regenerate after surgery is essential for treatment decision-making and prognosis evaluation.

Several methods have been used to evaluate liver regeneration. Volumetric computed tomography (CT) analysis directly reflects the volume of the remnant liver after hepatectomy (11,12) and is an intuitive method to assess postoperative liver regeneration in clinical practice. However, single volumetric CT analysis can only show general morphological changes of the remnant liver after surgery, and cannot predict liver regeneration capacity preoperatively, with a substantial hysteresis. Marker of proliferation Ki-67 (Ki-67) has been identified as a molecular marker for assessment of the cell proliferation index (13), and based on liver samples can evaluate the capacity of liver regeneration (14). Nevertheless, inherent limitations, including the need for invasive procedures and sampling error, limit its utility. Accordingly, a more effective and repeatable method is required to evaluate the regeneration capacity of the liver before surgery.

Magnetic resonance elastography (MRE) has shown to be a powerful tool for the staging of liver fibrosis and is currently the most accurate noninvasive imaging technology for this condition (15-18). It has the advantage of identifying early fibrosis, even when anatomical features suggestive of fibrosis are absent (17). Previous studies have shown that the severity of liver fibrosis and cirrhosis is closely related to postoperative regeneration of the remnant liver (19) and that both have negative effects on liver regeneration (20). A study by Jang *et al.* (21) confirmed that liver stiffness (LS) values measured at preoperative MRE were negatively correlated with the regeneration capacity of remnant liver after major hepatectomy, and that only the parenchymal hepatic resection rate (PHRR), defined as the resected liver volume as a percentage of total liver volume without volume of tumor and intrahepatic blood vessels, was a statistically significant factor for the liver regenerative index in multivariate analysis. However, although LS values showed a tendency towards a negative correlation with the regeneration index (RI), there was no statistical significance. Although PHRR may affect the regeneration process after hepatectomy (22), previous studies of liver regeneration have focused on major hepatectomy which was accompanied with high PHRR (21,23,24), which may underestimate the impact of differences in the microstructure of the liver itself (e.g., degree of liver fibrosis) on liver regeneration. Thus, the optimal range of PHRR to evaluate the effect of LS values on liver regeneration remains undetermined.

The purpose of this study was to predict the capacity of liver regeneration in patients with HCC after partial hepatectomy (PH) using LS values from MRE. Additionally, based on the effect of PHRR, we performed subgroup analysis, estimated the impact of the LS values on liver regeneration, and identified the optimal range of PHRRs. We present the following article in accordance with the Standards for Reporting of Diagnostic Accuracy Studies (STARD) reporting checklist (available at https://qims.amegroups.com/article/view/10.21037/qims-22-306/rc).

Methods

Participants

The study was conducted in accordance with the Declaration of Helsinki (as revised in 2013) and was approved by the institutional review board of the West China Hospital of Sichuan University. As a retrospective analysis, individual consent was waived. Between September 2018 and May 2021, a total of 163 patients with a pathologically confirmed diagnosis of HCC who underwent hepatectomy and preoperative routine magnetic resonance (MR) and MRE examinations were consecutively enrolled. Among them, 109 patients were excluded (*Figure 1*) due to the following exclusion criteria: (I) no follow-up contrast-enhanced CT (n=55); (II) no preoperative contrast-enhanced CT image taken within the 4 weeks prior to surgery (n=28); (III) liver resection performed more than 4 weeks after MR examination (n=4); (IV) images with severe motion and artifacts that limited the assessment (n=6); (V) diffuse intrahepatic recurrence or metastasis on postoperative CT that influenced the measurement of

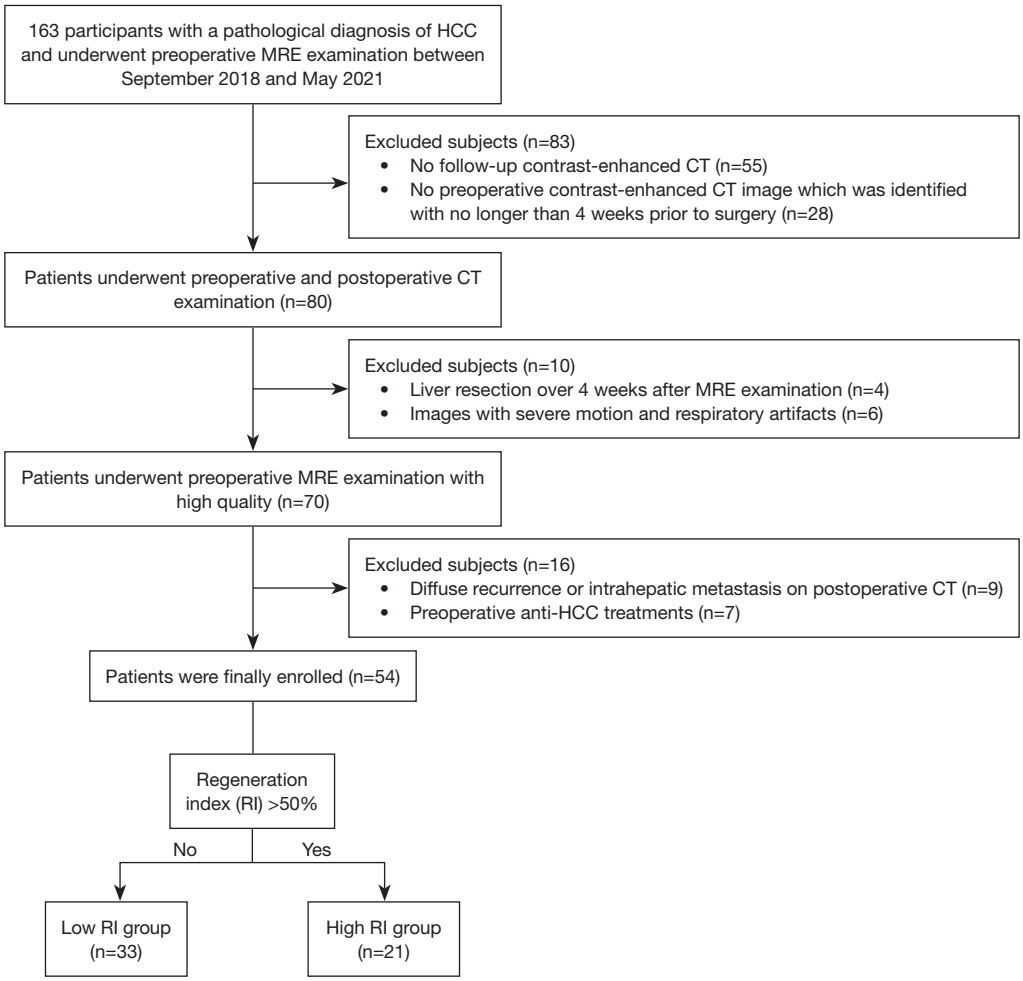

Figure 1 Flow diagram of the study population. HCC, hepatocellular carcinoma; MRE, magnetic resonance elastography; CT, computed tomography; RI, regeneration index.

remnant liver volume (n=9); or (VI) a history of TACE, chemotherapy, or other antitumor therapy before surgery (n=7). Thus, 54 patients were included in the final analysis.

MRE

All MRE examinations were performed on a 3.0 T MR system (Discovery MR 750w, GE Healthcare, Chicago, IL, USA) with a 16-channel torso phased-array coil (GE Medical System, USA). All patients were placed in the supine position, with a passive pneumatic driver secured with an elastic belt wrapped around the anterior body wall close to the right hepatic lobe. The active acoustic driver outside the scanner room produced continuous shear waves at 60 Hz, which were transmitted via a polyvinyl chloride tube to the passive driver into the deep liver.

This two-dimensional (2D) spin-echo echo-planar (SE-EP) MRE sequence was accompanied by 4 contiguous axial slices taken through the widest portion of the liver and imaged sequentially. Patients were requested to hold their breath for approximately 16 seconds. The LS maps were automatically generated from the wave information using an inversion algorithm, and a confidence map was overlaid on the stiffness maps to exclude regions that were noisy and had less reliable stiffness data, which guided the region of interest (ROI) selection.

Routine MR imaging sequences included in the standardized scanning protocol were respiratory-triggered axial T2-weighted fast recovery fast spin echo sequences, in and out of phase T1-weighted imaging acquired with fast

spoiled gradient-recalled dual-echo sequences, and pre- and post-contrast liver acceleration volume acquisition (LAVA) acquired with gradient recalled echo sequences in the arterial phase (20 s), portal venous phase (60 s), and delayed phase (180 s). The detailed parameters of each sequence are summarized in Table S1.

Measurements of LS values

All MRE images were analyzed by two independent radiologists (AA, BB, with 10- and 6-year of experience in reading MR images, respectively), who were blinded to the clinical information, laboratory tests, and histopathological results. For each patient, future remnant liver parenchyma was chosen by referring to the postoperative CT image for the ROI measurement. The ROIs were drawn manually on as much of the liver as possible that had substantial wave propagation based on the MRE magnitude, wave, and stiffness images, while excluding the major blood vessels and areas close to the liver boundary. The mean value of the 4 ROIs was used for further analysis. The mechanical property measured with MRE was the magnitude of the complex shear modulus expressed in kPa.

CT techniques

All patients underwent contrast-enhanced abdominal CT using Revolution CT (GE Healthcare) or SOMATOM definition (Siemens Healthineers, Erlangen, Germany) systems. The CT examinations were performed before and after intravenous administration of iodinated contrast material, with arterial (30–35 s) and portal venous (60–70 s) phases. The following parameters were used: tube voltage, 100 or 120 kVp; tube current, 200–450 mA; slice thickness, 1.5–5 mm; pitch, 0.992:1; rotation speed: 0.5 s/rot; and adaptive statistical iterative reconstruction-V (ASIR-V): 20%. All patients received an intravenous nonionic contrast agent (iodine concentration, 370 mg/mL; volume, 1.5–2.0 mL/kg of body weight; contrast type, iopromide injection, Bayer Pharma AG) at a rate of 2–3 mL/s, and a 20 mL flush of normal saline was administered immediately after the contrast injection.

Preoperative CT liver volume

The volume of preoperative future liver remnant (LVpre) on preoperative CT was measured using image processing software (United Imaging Workstation; United Imaging Healthcare, Shanghai, China), and CT images obtained during the portal phase were used for volume analysis. Initially, the entire liver parenchyma and vessels (including the hepatic portal vein, hepatic vein, and their main branches) were automatically extracted after the CT images were loaded into the software, and manual corrections of the liver contours were applied by the user (AA, with 10-year of abdominal CT experience), who was blinded to the clinical information, MRE data, laboratory tests, and histopathological results, where necessary. In the second step, the user drew a straight line along the maximum diameter of the tumor, and the tumor was semiautomatically segmented. The volume of the total functional liver (removing tumor volume and vessel volume) was automatically calculated and displayed. In the third step, a virtual curve was drawn by the user along the surgical margin with reference to the postoperative CT image. Eventually, the LVpre (removing the volume of blood vessels) was calculated automatically.

Postoperative CT liver volume

As it is not known when liver regeneration is complete, its evaluation was performed by previous studies at highly variable postoperative periods, such as 1–6 months after surgery (25,26). As the remnant liver volume often has significantly regenerated by the 6th month following hepatectomy, although the timing of follow-up CT varied due to the retrospective nature of the study, images in the portal phase closest to the 6th month postoperatively were selected to calculate the volume of postoperative liver remnant (LVpost). The procedure of the remnant liver parenchyma and major intrahepatic vessel extraction was similar to the above description, and the LVpost (removing volume of vessels) was automatically calculated.

The following ratios were calculated: (I) the RI expressed as:

$$RI = \frac{LVpost - LVpre}{LVpre} \times 100\% \quad [1]$$

and (II) the degree of PHRR (22), calculated as:

$$PHRR = \frac{(Volume\ of\ the\ total\ functional\ liver) - LVpre}{Volume\ of\ the\ total\ functional\ liver} \times 100\% \quad [2]$$

Additionally, the cutoff value of RI was determined to be 50% (23). Participants were classified into two groups: a high RI group with values above the cutoff and a low RI group with values below the cutoff.

Histopathologic analysis

The diagnosis of liver fibrosis was confirmed by the histology of the resected specimens. One pathologist, who was blinded to the imaging results and patient data, independently reviewed the resection specimens to evaluate the degrees of liver fibrosis using the METAVIR scoring system (27), where F0 represents no fibrosis, F1 represents portal fibrosis without septa, F2 represents portal fibrosis and few septa, F3 represents numerous septa without cirrhosis, and F4 represents cirrhosis. In agreement with the previous classification methods (28), all participants were classified into three groups: The no-to-mild (F0–1) group, moderate-to-advanced (F2–3) group, and severe fibrosis or cirrhosis (F4) group.

Definition of posthepatectomy liver failure (PLF)

According to the grading system of the International Study Group of Liver Surgery (ISGLS), PLF was defined as increased INR and hyperbilirubinemia based on the normal range of cut-off levels of the local laboratory on or after postoperative day (POD) 5. In patients with preoperatively increased INR or increased serum bilirubin concentration, PLF was defined by an increasing serum bilirubin concentration and increasing INR on or after POD 5 compared with the values of the previous day (29).

Statistical analysis

Continuous variables were expressed as the means ± standard deviations, and categorical variables were presented as frequencies and proportions. The differences in the baseline characteristics between the low and high RI groups, between patients with and without liver failure, were tested with the independent sample *t*-test or Mann-Whitney U test for continuous variables and the chi-square test, Fisher's exact test, or Wilcoxon rank-sum test for categorical variables. All participants were divided into three subgroups based on the value of PHRR: low PHRR (<30%) group, intermediate PHRR (30–50%) group, and high PHRR (>50%) group. Baseline characteristics among the three subgroups were compared using analysis of variance (ANOVA) or the Kruskal-Wallis test for continuous variables and the chi-squared test or Fisher's exact test or Wilcoxon rank-sum test for categorical variables. Bonferroni corrections were then performed for the multiple pairwise comparisons, and the intraclass correlation coefficient (ICC) with the two-way random method was used in the analysis of interobserver agreement of the LS values. The agreement between measurements was interpreted using the following guidelines: greater than 0.90 implied excellent agreement, 0.75–0.90 implied good agreement, 0.50–0.75 implied moderate agreement, and less than 0.50 implied poor agreement (30). Univariate and multivariate logistic regression analyses were performed to identify the risk factors for high RI and for liver failure, and only those factors with statistical significance (P<0.05) by univariate analysis were entered into the multivariate logistic regression analysis. The variance inflation factor (VIF) was used to determine the presence of multicollinearity among the multiple variables in the multivariate logistic regression model, and a P value under 10 indicated an acceptable model. Receiver operating characteristic (ROC) curves were plotted, and the areas under the curve (AUCs) of the LS values were calculated. The cutoff point was selected at the maximized value of the Youden index, and sensitivity and specificity were calculated for this cutoff value. Correlations of PHRR and LVpre, PHRR and type of hepatectomy, LS value and fibrosis stage, fibrosis stage and the value of RI, baseline characteristics and the value of RI, and LS value and the value of RI were assessed using the Spearman correlation test. All statistical tests were performed using the software SPSS 26 (IBM Corp., Armonk, NY, USA) and R software (version 4.0.2; The R Foundation for Statistical Computing, Vienna, Austria), and P values less than 0.05 were considered significant.

Results

Baseline characteristics of the patient cohort

The baseline characteristics of participants are displayed in *Table 1*. A total of 54 HCC patients with a mean age of 51.13 (range, 29 to 74) years were included, and the follow-up period from surgery to postoperative CT scans ranged from 22 to 333 days. Of the total cohort, there were 33 patients (28 men and 5 women) in the low RI group and 21 (18 men and 3 women) in the high RI group. The LVpre, PHRR, and albumin (ALB) of the HCC patients showed a significant difference between the low RI group and the high RI group (LVpre: 872.81±193.33 *vs.* 518.22±116.73 cm^3, P<0.001; PHRR: 26.86%±16.49% *vs.* 53.52%±10.47%, P<0.001; ALB: 39.97±5.41 *vs.* 44.06±4.76 g/L, P<0.002). In addition, the proportion of patients receiving major hepatectomy, which was defined as resection of 3 or more

Table 1 Comparison of baseline characteristics of patients with low RI and high RI

Baseline characteristics	Low RI (n=33)	High RI (n=21)	P value
Age (years)	51.36±10.95	50.76±11.43	0.979
Gender			0.930
Male	28 (84.85)	18 (85.71)	
Female	5 (15.15)	3 (14.29)	
RI (%)	21.36±12.34	90.92±50.87	<0.001*
PHRR (%)	26.86±16.49	53.52±10.47	<0.001*
LVpre (cm^3)	872.81±193.33	518.22±116.73	<0.001*
LVpost (cm^3)	1,055.07±173.11	960.13±183.55	0.060
BMI (kg/m^2)	23.40±3.73	23.04±2.75	0.707
Tumor size (cm)	5.31±3.59	6.66±3.68	0.188
Multifocality	8 (24.24)	9 (42.86)	0.151
ALT (IU/L)	99.73±250.37	104.19±183.95	0.073
AST (IU/L)	131.33±363.84	92.48±179.00	0.116
ALP (IU/L)	94.88±46.84	109.48±31.43	0.214
GGT (IU/L)	90.18±76.11	121.29±78.77	0.075
AST/ALT	1.11±0.32	1.01±0.45	0.319
TP (g/L)	68.09±8.59	69.46±8.67	0.385
ALB (g/L)	39.97±5.41	44.06±4.76	0.002*
TBIL (μmol/L)	14.89±6.80	13.51±5.30	0.204
DBIL (μmol/l)	5.53±3.86	4.892±2.55	0.275
HGB (g/L)	142.03±24.45	139.52±16.47	0.472
PLT (10^9/L)	137.79±67.06	179.29±83.71	0.056
PT (s)	12.88±4.34	12.71±4.68	0.790
INR	1.04±0.16	1.04±0.11	0.434
HBsAg (positive)	30 (90.91)	19 (90.48)	0.957
HBeAg (positive)	3 (9.09)	0 (0.00)	0.274
Anti-HCV (positive)	1 (3.03)	0 (0.00)	1.000
Cirrhosis	25 (75.76)	16 (76.19)	0.971
Ascites	0 (0.00)	1 (4.76)	0.389
High blood pressure	8 (24.24)	4 (19.05)	0.654
Diabetes mellitus	0 (0.00)	3 (14.29)	0.054
BCLC stage			0.463
0	1 (3.03)	1 (4.76)	
A	20 (60.60)	10 (47.62)	
B	9 (27.27)	7 (33.33)	
C	3 (9.09)	3 (14.29)	

Table 1 *(continued)*

Table 1 *(continued)*

Baseline characteristics	Low RI (n=33)	High RI (n=21)	P value
ALBI grade			0.165
I	24 (72.73)	19 (90.48)	
II	7 (21.21)	2 (9.52)	
III	2 (6.06)	0 (0.00)	
Type of hepatectomy			<0.001*
Minor (<3 Couinaud segments)	28 (84.85)	2 (9.52)	
Major (≥3 Couinaud segments)	5 (15.15)	19 (90.48)	
Fibrosis stage			0.003*
F0–1	2 (6.06)	8 (38.10)	
F2–3	17 (51.52)	10 (47.62)	
F4	14 (42.42)	3 (14.28)	
Inflammation grade			0.526
G1	2 (6.06)	2 (9.52)	
G2	16 (48.48)	8 (38.10)	
G3	15 (45.45)	11 (52.39)	
LS value (kPa)	5.02±1.16	3.08±1.20	<0.001*

Data are represented in mean ± SD or n (%). Data were evaluated by independent *t*-test or Mann-Whitney U test for continuous variables and chi-square test or Fisher's exact test or Wilcoxon rank-sum test for categorical variables. *, P<0.05. RI, regeneration index; PHRR, parenchymal hepatic resection rate; LVpre, volume of preoperative future liver remnant; LVpost, volume of postoperative liver remnant; BMI, body mass index; ALT, alanine aminotransferase; AST, aspartate aminotransferase; ALP, alkaline phosphatase; GGT, γ-glutamyl transferase; TP, total protein; ALB, albumin; TBIL, total bilirubin; DBIL, direct bilirubin; HGB, hemoglobin; PLT, platelet count; PT, prothrombin time; INR, international normalized ratio; HBsAg, hepatitis B surface antigen; HBeAg, hepatitis B e antigen; anti-HCV, hepatitis C virus antibody; BCLC, Barcelona Clinic Liver Cancer; ALBI, albumin-bilirubin; LS, liver stiffness.

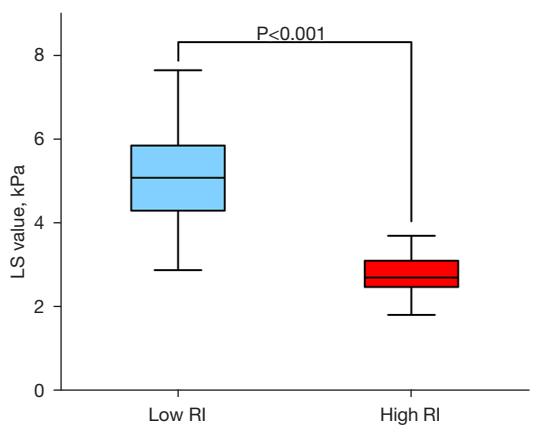

Figure 2 Comparison of LS values at MRE between patients with high RI and low RI. LS, liver stiffness; RI, regeneration index; MRE, magnetic resonance elastography.

Couinaud segments, was significantly lower in the low RI group than the high RI group (15.15% *vs.* 90.48%, P<0.001).

LS value at MRE in distinguishing high RI from low RI

Agreement between the two radiologists was excellent for the LS value [ICC, 0.934; 95% confidence interval (CI): 0.889 to 0.961]. Moreover, LS values at MRE increased in the low RI group compared with the high RI group (5.02±1.16 *vs.* 3.08±1.20 kPa, P<0.001, *Figure 2*). An optimal cutoff value of 3.30 kPa was used to divide all participants into a high RI group (*Figure 3*) and low RI group (*Figure 4*) with an AUC value of 0.882 (95% CI: 0.767 to 0.996), sensitivity of 80.95%, and specificity of 93.94% (*Figure 5*).

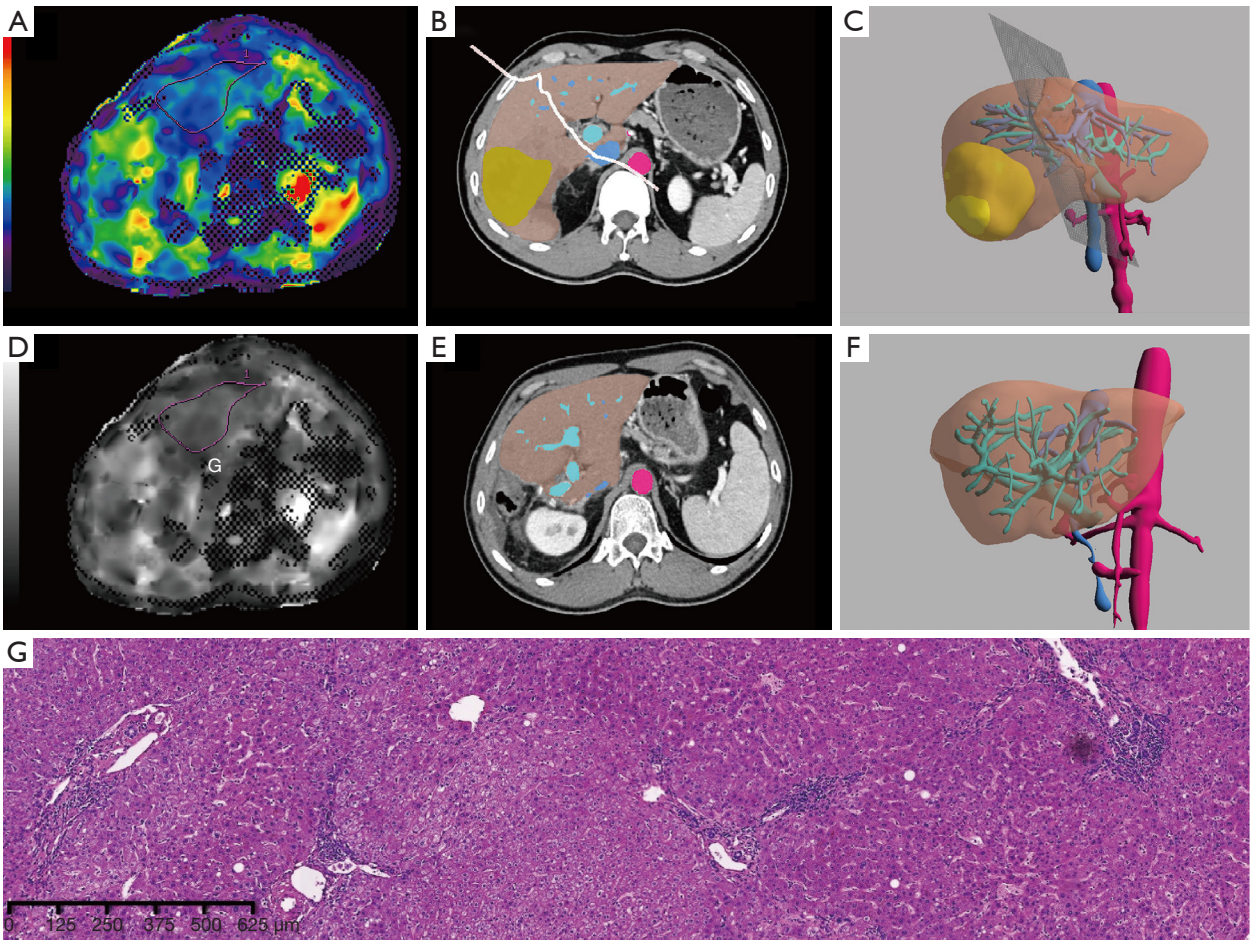

Figure 3 A 50-year-old male HCC patient with a high RI. (A) Elastogram (color scale) with confidence map. The average LS value for the unresected lesion-free area in the left lobe of the liver was 2,706.5 kPa, with an individual ROI of 2,850 mm^2. (B) Simulation of surgical resection on the portal venous phase of the CT image before hepatectomy, with a PHRR of 55.00%. (C) 3D image of the preoperative simulated resection. (D) Elastogram (grayscale) with confidence map. (E) The axial CT image of the actual remnant liver on the third month after surgery. (F) 3D image of the actual remnant liver on the third postoperative month. (G) The fibrosis stage of the lesion-free area was histopathologically proven to be F1 with HE staining at 4× magnification. HCC, hepatocellular carcinoma; RI, regeneration index; LS, liver stiffness; ROI, region of interest; CT, computed tomography; PHRR, parenchymal hepatic resection rate; 3D, three-dimensional; HE, hematoxylin-eosin.

Univariate and multivariate analyses

In addition to ALB [odds ratio (OR), 1.232; 95% CI: 1.039 to 1.461; P=0.017] and PHRR (OR, 1.128; 95% CI: 1.062 to 1.199; P<0.001), lower LS values (OR, 0.267; 95% CI: 0.137 to 0.522; P<0.001) were identified as significant predictors of high RI in univariate analysis. Due to the strong correlation between PHRR and LVpre (r=−0.769; P<0.001) (Figure S1A) and between PHRR and the type of hepatectomy (r=0.846; P<0.001) (Figure S1B), only PHRR was included in the multivariate analysis. The multivariate analysis also revealed lower LS values at MRE were still associated with greater odds of high RI (OR, 0.049; 95% CI: 0.002 to 0.980) (*Table 2*). The VIF value of all 3 parameters included in the multivariate analysis was under 10, indicating no multicollinearity had occurred in the multivariate model.

Subgroup analysis

Considering the significant impact of PHRR on RI, in the

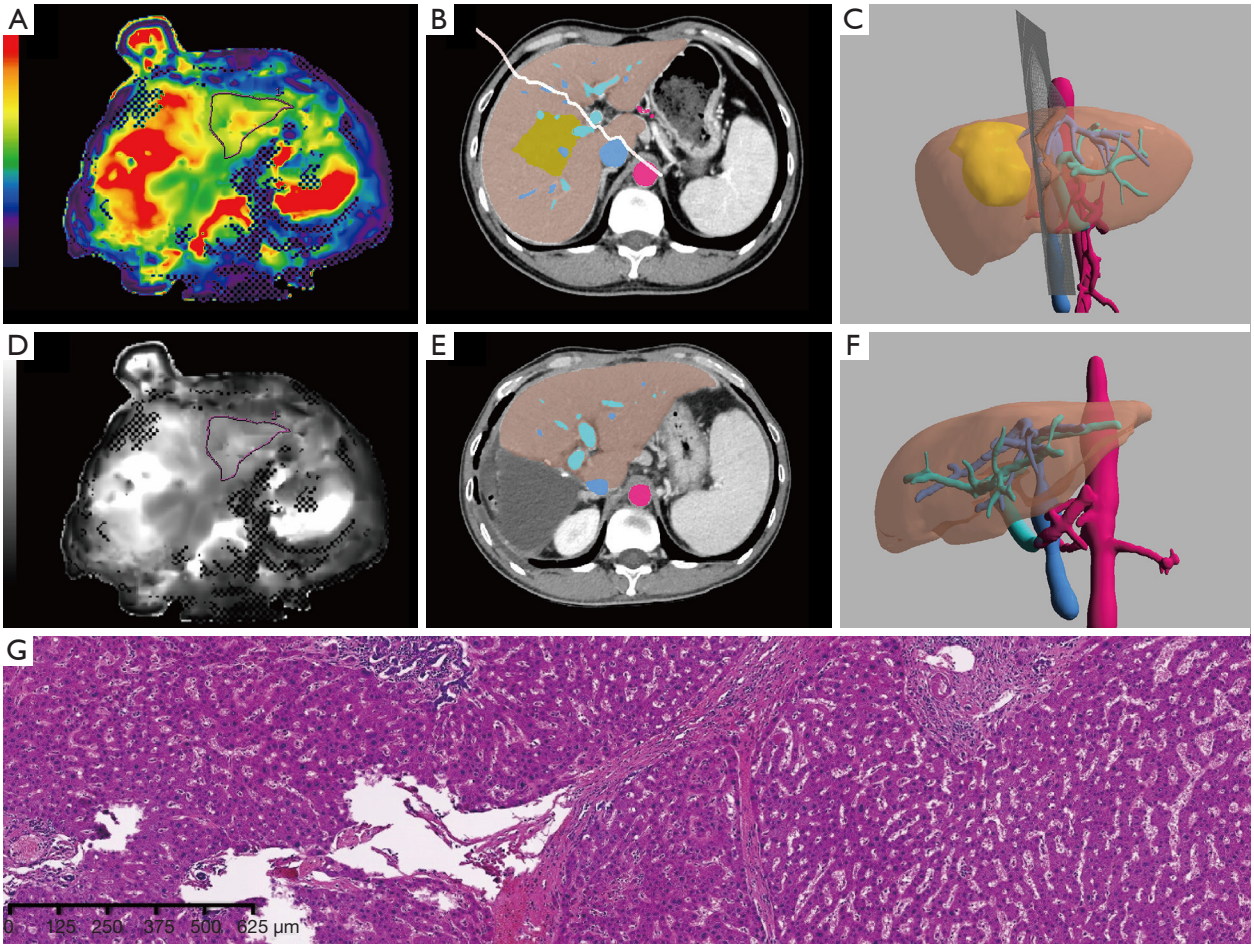

Figure 4 A 41-year-old male HCC patient with a low RI and postoperative liver failure. (A) Elastogram (color scale) with confidence map. The average LS value for the unresected lesion-free area in the left lobe of the liver was 4,651.3 kPa, with an individual ROI of 2,412 mm^2. (B) Simulation of surgical resection on the portal venous phase of the CT image before hepatectomy, with a PHRR of 58.26%. (C) 3D image of the preoperative simulated resection. (D) Elastogram (grayscale) with confidence map. (E) The axial CT image of the actual remnant liver on the third month after surgery. (F) 3D image of the actual remnant liver on the third postoperative month. (G) The fibrosis stage of the lesion-free area was histopathologically shown to be F4 with HE staining at 4× magnification. HCC, hepatocellular carcinoma; RI, regeneration index; LS, liver stiffness; ROI, region of interest; CT, computed tomography; PHRR, parenchymal hepatic resection rate; 3D, three-dimensional; HE, hematoxylin-eosin.

present study, patients were divided into three subgroups according to the value of PHRR (31): a low PHRR (<30%) group (n=21), intermediate PHRR (30–50%) group (n=17), and high PHRR (>50%) group (n=16). Significant differences were observed among the three subgroups when considering the value of RI, PHRR, LVpre, and type of hepatectomy (all P<0.001), yet other baseline characteristics were not different (all P>0.05) (Table S2).

In the low and high PHRR groups, there was no significant relationship (all P>0.05) between RI and LS values of MRE (Table S3). However, a negative relationship (r=–0.799; P<0.001) was shown between LS values and RI in the intermediate PHRR group. When dividing the intermediate PHRR subgroup into two groups according to the cutoff value of RI (50%), higher LS values were also found in participants with low RI compared with those with high RI (5.56±1.15 *vs.* 2.51±0.46 kPa, P<0.001) (Figure S2). The detailed comparison of baseline characteristics between patients with low and high RI in the intermediate PHRR group is summarized in Table S4.

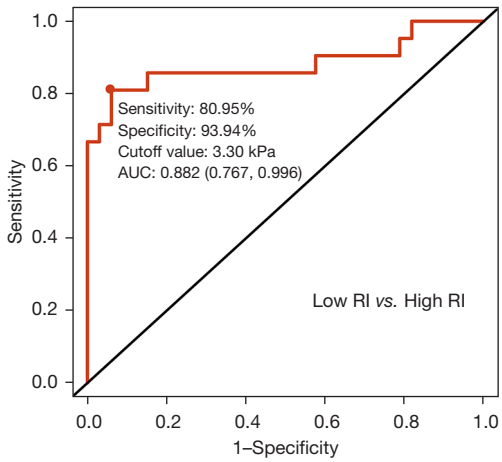

Figure 5 ROC curves of LS value to distinguish HCC patients with high RI and low RI. AUC, area under the curve; RI, regeneration index; ROC, receiver operating characteristic; LS, liver stiffness; HCC, hepatocellular carcinoma.

Relationship between LS values, liver fibrosis, and liver regeneration

In all participants, the LS values of MRE showed significant positive correlations with fibrosis stage (r=0.699; P<0.001; Figure S3A). Accordingly, more serious hepatic fibrosis was found in the low RI group than in the high RI group (F0–1: 6.06% *vs.* 38.10%, F2–3: 51.52% *vs.* 47.62%, F4: 42.42% *vs.* 14.28%, P=0.003; Figure S3B).

In the intermediate PHRR subgroup, significant positive correlations were shown between the LS values of MRE and the fibrosis stage (r=0.670; P=0.003; Figure S4A), and more serious hepatic fibrosis was observed in patients with a low RI than with a high RI (F0–1: 0% *vs.* 51.14%, F2–3: 40.00% *vs.* 42.86%, F4: 60.00% *vs.* 0.00%; P=0.002; Figure S4B).

PLF according to the ISGLS grading system

Increased international normalized ratio (INR) and elevated levels of serum bilirubin on or after POD 5 were seen in 17 participants (31.48%), fulfilling the criteria for PLF proposed by the ISGLS. The PHRR was significantly different in participants with and without PLF (46.04%±20.17% *vs.* 33.18%±17.93%, P=0.022), and higher LS values of MRE were also seen in the 17 patients with PLF compared with those without PLF (4.97±1.28 *vs.* 3.94±1.51 kPa, P=0.018; *Figure 6A*). An optimal cutoff value of 5.06 kPa was used to divide all participants into two groups (patients with PLF and without PLF) with an AUC value of 0.709 (95% CI: 0.563 to 0.855), sensitivity of 64.71%, and specificity of 75.68% (*Figure 6B*). As previously stated, a significant positive correlation was found between the LS values of MRE and fibrosis stage (r=0.699; P<0.001; *Figure 6C*), and more serious hepatic fibrosis was also found in patients with PLF than in those without PLF (F0–1: 5.88% *vs.* 24.32%, F2–3: 35.29% *vs.* 56.76%, F4: 58.82% *vs.* 18.92%, P=0.004; *Figure 6D*). The detailed information of baseline characteristics between patients with and without PLF is shown in *Table 3*. Multivariate analysis also revealed that except for higher PHRR (OR, 1.062; 95% CI: 1.015 to 1.112), higher LS values at MRE were still associated with greater odds of PLF (OR, 2.055; 95% CI: 1.238 to 3.410) (*Table 4*).

Discussion

The present study investigated the feasibility of using LS values measured with MRE for assessing liver regeneration in patients with HCC after hepatic resection, and the findings indicated that lower LS values have a significant association with high RI in univariate analysis. Moreover, multivariate analysis also revealed that lower LS values correlated significantly with high RI and yielded good diagnostic performance for the preoperative assessment of liver regenerative capacity.

Previous studies have demonstrated MRE as a useful noninvasive diagnostic technique for detecting hepatic fibrosis, and LS values can be used to identify the grade of liver fibrosis (32,33). The basic principle of MRE is to propagate mechanically produced shear waves into the liver which propagate more rapidly in stiffer tissue than in softer tissue. If the shear waves are continuously produced, the speed of propagation is reflected in its wavelength, and as tissue stiffness increases, the wavelength becomes more elongated (17,34). This means that the greater the LS values, the higher the degree of liver fibrosis. Furthermore, some studies have suggested the degree of liver fibrosis can affect preoperative liver functional reserve, with a negative impact on postoperative remnant liver regeneration (35,36). Jang *et al.* (21) reported that LS values measured at preoperative MRE were negatively associated with the regeneration capacity of the remnant liver after right hepatectomy, which is consistent with our findings.

There are two possible reasons for the lower regeneration capacity of fibrotic livers. First, telomere shortening in fibrotic hepatocytes results in the failure of cell replication during the progression of liver cirrhosis (37-39), which may

Table 2 Univariate and multivariate analyses of the risk factors of RI status

Variables	Univariate		Multivariate	
	OR (95% CI)	P value	OR (95% CI)	P value
Age (years)	0.995 (0.946, 1.046)	0.844		
Gender				
Male	Reference			
Female	0.933 (0.198, 4.393)	0.93		
PHRR (%)	1.128 (1.062, 1.199)	<0.001*	1.206 (1.043, 1.393)	0.011*
BMI (kg/m^2)	0.968 (0.821, 1.142)	0.701		
Tumor size (cm)	1.109 (0.949, 1.295)	0.194		
Multifocality	2.344 (0.724, 7.590)	0.155		
ALB (g/L)	1.232 (1.039, 1.461)	0.017*	1.636 (0.916, 2.920)	0.096
ALT (IU/L)	1.000 (0.998, 1.003)	0.943		
AST (IU/L)	1.000 (0.997, 1.002)	0.650		
ALP (IU/L)	1.009 (0.995, 1.023)	0.228		
GGT (IU/L)	1.005 (0.998, 1.013)	0.161		
AST/ALT	0.451 (0.095, 2.130)	0.315		
TP (g/L)	1.020 (0.954, 1.089)	0.564		
TBIL (μmol/L)	0.961 (0.870, 1.061)	0.431		
DBIL (μmol/L)	0.929 (0.762, 1.134)	0.470		
HGB (g/L)	0.995 (0.969, 1.020)	0.675		
PLT (10^9/L)	1.008 (1.000, 1.016)	0.062		
PT (s)	0.991 (0.873, 1.125)	0.893		
INR	1.172 (0.023, 59.274)	0.937		
HBsAg (positive)	0.983 (0.150, 6.443)	0.983		
Cirrhosis	1.024 (0.284, 3.688)	0.971		
High blood pressure	0.735 (0.191, 2.834)	0.655		
BCLC stage				
0	Reference			
A	0.500 (0.028, 8.853)	0.636		
B	0.778 (0.041, 14.750)	0.867		
C	1.000 (0.041, 24.547)	1.000		
ALBI grade				
I	Reference			
II	0.361 (0.067, 1.942)	0.235		
III	–	–		
LS value (kPa)	0.267 (0.137, 0.522)	<0.001*	0.049 (0.002, 0.980)	0.048*

*, referred to P<0.05. RI, regeneration index; PHRR, parenchymal hepatic resection rate; BMI, body mass index; ALB, albumin; ALT, alanine aminotransferase; AST, aspartate aminotransferase; ALP, alkaline phosphatase; GGT, γ-glutamyl transferase; TP, total protein; TBIL, total bilirubin; DBIL, direct bilirubin; HGB, hemoglobin; PLT, platelet count; PT, prothrombin time; INR, international normalized ratio; HBsAg, hepatitis B surface antigen; BCLC, Barcelona Clinic Liver Cancer; ALBI, albumin-bilirubin; LS, liver stiffness; OR, odds ratio; CI, confidence interval.

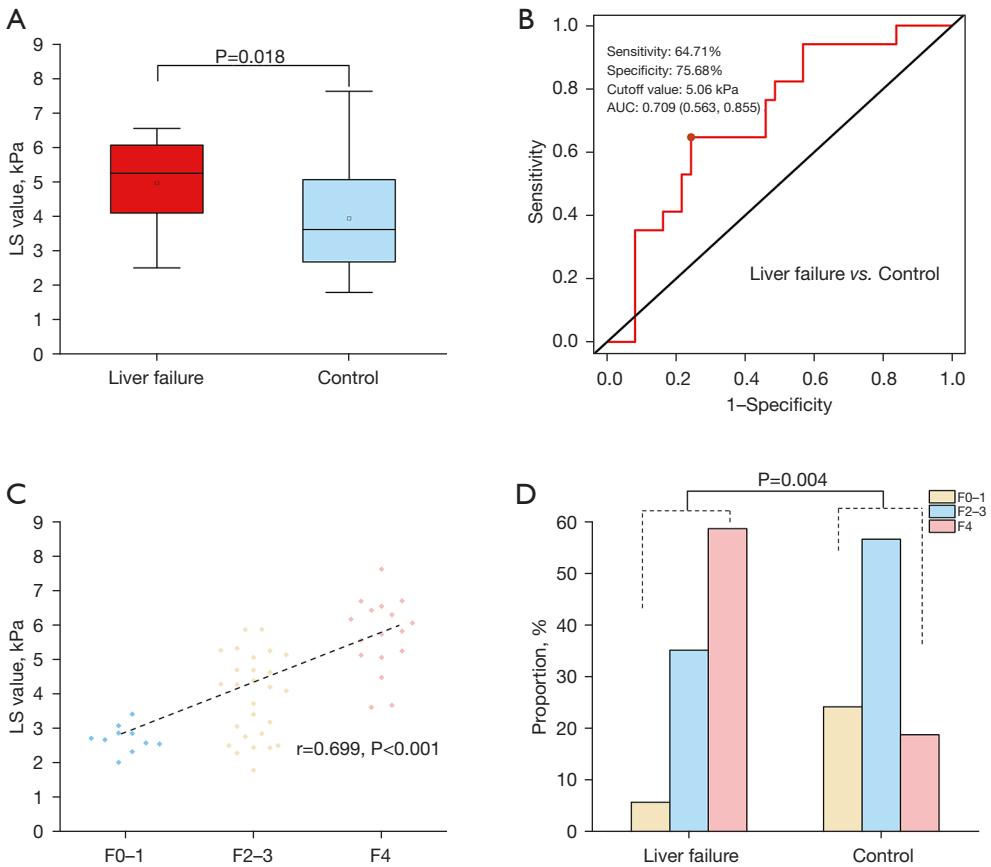

Figure 6 Relationship between LS values, liver fibrosis, and liver failure. (A) Comparison of LS values at MRE between patients with and without postoperative liver failure. (B) ROC curves of LS value to distinguish HCC patients with and without postoperative liver failure. (C) LS values between patients with different fibrosis stage. (D) Comparison of fibrosis stage between patients with and without postoperative liver failure. LS, liver stiffness; AUC, area under the curve; MRE, magnetic resonance elastography; ROC, receiver operating characteristic; HCC, hepatocellular carcinoma.

limit the regenerative capacity. Second, the differential recruitment of pro-regenerative CXCR7/Id1 *vs.* pro-fibrotic FGFR1/CXCR4 angiocrine pathways in the vascular niche balances regeneration and fibrosis. In response to liver injury, increased CXCR7 in liver sinusoidal cells stimulates regeneration, but suppression of CXCR7 function stimulates CXCR4 and causes liver fibrosis as opposed to regeneration (40).

Notably, apart from the abovementioned LS values, PHRR was confirmed to be a powerful predictor of RI in both univariate and multivariate analyses, consistent with the results of Kele *et al.* (22). This may be because as the rate of liver resection increases, the amount of remnant liver parenchyma decreases, and the reserve function of the remnant liver cannot meet the metabolic demand of the liver. This stimulates urgent liver regeneration, and the relatively large space for regeneration of the remnant liver after surgery also stimulates the rapid growth of liver tissue. In addition, the postoperative decrease in remnant liver parenchyma will lead to an increase in the proportion of blood flow into the liver as well as an increase in the concentration of cytokines, both of which will promote remnant liver regeneration (31,41).

In our study, the LVpre, PHRR, and type of hepatectomy all showed statistically significant differences between the low RI group and the high RI group. However, both LVpre and type of hepatectomy had a high correlation with PHRR, which also concurs with the findings of Kele *et al.* (22). Additionally, the type of hepatectomy or LVpre, compared with the PHRR, could not fully reflect the resection information of the liver owing to the variability in size of the various liver segments among the patients (42).

Table 3 Comparison of baseline characteristics of patients with and without postoperative liver failure

Baseline characteristics	Liver failure (n=17)	Control (n=37)	P value
Age (years)	50.53±14.19	51.41±9.47	0.789
Gender			0.988
Male	15 (88.23)	31 (83.78)	
Female	2 (11.76)	6 (16.22)	
RI (%)	55.67±63.71	45.08±38.18	0.451
PHRR (%)	46.04±20.17	33.18±17.93	0.022*
LVpre (cm^3)	704.33±289.01	748.97±218.75	0.689
LVpost (cm^3)	1,045.43±226.15	1,005.61±159.14	0.429
BMI (kg/m^2)	23.24±4.11	23.27±3.02	0.980
Tumor size (cm)	6.33±3.69	5.61±3.66	0.507
Multifocality	7 (41.18)	10 (27.03)	0.353
ALT (IU/L)	42.24±25.93	128.68±267.97	0.060
AST (IU/L)	40.82±26.97	150.86±363.00	0.075
ALP (IU/L)	94.65±27.23	103.27±47.13	0.410
GGT (IU/L)	96.35±49.41	105.00±88.50	0.648
AST/ALT	1.03±0.29	1.09±0.41	0.607
TP (g/L)	70.09±6.99	67.95±9.20	0.351
ALB (g/L)	42.82±4.89	40.98±5.73	0.232
TBIL (μmol/L)	15.81±8.57	13.68±4.83	0.351
DBIL (μmol/l)	5.85±4.94	4.98±2.44	0.497
HGB (g/L)	145.18±22.34	139.16±21.23	0.358
PLT (10^9/L)	150.53±84.28	155.49±73.07	0.836
PT (s)	12.92±4.32	13.77±4.54	0.903
INR	1.05±0.12	1.03±0.15	0.710
HBsAg (positive)	16 (94.12)	33 (89.19)	1.000
HBeAg (positive)	1 (5.88)	2 (5.41)	1.000
Anti-HCV (positive)	1 (5.88)	0 (0.00)	0.315
Cirrhosis	15 (88.24)	26 (70.27)	0.152
Ascites	1 (5.88)	0 (0.00)	0.876
High blood pressure	4 (23.53)	8 (21.62)	0.981
Diabetes mellitus	2 (11.76)	1 (2.70)	0.177
BCLC stage			0.145
0	0 (0.00)	2 (5.41)	
A	8 (4.71)	22 (59.46)	
B	6 (35.29)	10 (27.03)	
C	3 (17.65)	3 (8.11)	

Table 3 *(continued)*

Table 3 *(continued)*

Baseline characteristics	Liver failure (n=17)	Control (n=37)	P value
ALBI grade			0.790
I	14 (82.35)	29 (78.38)	
II	2 (11.76)	7 (18.92)	
III	1 (5.88)	1 (2.70)	
Type of hepatectomy			0.149
Minor (<3 Couinaud segments)	7 (41.18)	23 (62.16)	
Major (≥3 Couinaud segments)	10 (58.82)	14 (37.84)	
Inflammation grade			0.053
G1	0 (0.00)	4 (10.81)	
G2	5 (29.41)	19 (51.35)	
G3	12 (70.59)	14 (37.84)	
Fibrosis stage			0.004*
F0–1	1 (5.88)	9 (24.32)	
F2–3	6 (35.29)	21 (56.76)	
F4	10 (58.82)	7 (18.92)	
LS value (kPa)	4.97±1.28	3.94±1.51	0.018*

Data are represented in mean ± SD or n (%). Data were evaluated by independent *t*-test or Mann-Whitney U test for continuous variables and chi-square test or Fisher's exact test for categorical variables. *, P<0.05. RI, regeneration index; PHRR, parenchymal hepatic resection rate; LVpre, volume of preoperative future liver remnant; LVpost, volume of postoperative liver remnant; BMI, body mass index; ALT, alanine aminotransferase; AST, aspartate aminotransferase; ALP, alkaline phosphatase; GGT, γ-glutamyl transferase; TP, total protein; ALB, albumin; TBIL, total bilirubin; DBIL, direct bilirubin; HGB, hemoglobin; PLT, platelet count; PT, prothrombin time; INR, international normalized ratio; HBsAg, hepatitis B surface antigen; HBeAg, hepatitis B e antigen; anti-HCV, hepatitis C virus antibody; BCLC, Barcelona Clinic Liver Cancer; ALBI, albumin-bilirubin; LS, liver stiffness.

Table 4 Univariate and multivariate analyses of the risk factors of postoperative liver failure

Variables	Univariate		Multivariate	
	OR (95% CI)	P value	OR (95% CI)	P value
Age (years)	0.993 (0.942, 1.046)	0.785		
Gender				
Male	Reference			
Female	0.689 (0.123, 3.838)	0.670		
PHRR (%)	1.038 (1.004, 1.073)	0.029*	1.062 (1.015, 1.112)	0.009*
BMI (kg/m^2)	0.998 (0.840, 1.186)	0.980		
Tumor size (cm)	1.054 (0.904, 1.230)	0.501		
Multifocality	1.890 (0.565, 6.326)	0.302		
ALB (g/L)	1.073 (0.950, 1.212)	0.259		

Table 4 *(continued)*

Table 4 *(continued)*

Variables	Univariate		Multivariate	
	OR (95% CI)	P value	OR (95% CI)	P value
ALT (IU/L)	0.993 (0.979, 1.008)	0.381		
AST (IU/L)	0.994 (0.981, 1.008)	0.418		
ALP (IU/L)	0.994 (0.979, 1.010)	0.483		
GGT (IU/L)	0.998 (0.991, 1.006)	0.703		
AST/ALT	0.654 (0.133, 3.204)	0.600		
TP (g/L)	1.032 (0.960.1.109)	0.392		
TBIL (μmol/L)	1.054 (0.962, 1.155)	0.261		
DBIL (μmol/L)	1.074 (0.910, 1.267)	0.398		
HGB (g/L)	1.014 (0.986, 1.043)	0.340		
PLT (10^9/L)	0.999 (0.991, 1.007)	0.822		
PT (s)	1.008 (0.887, 1.146)	0.902		
INR	2.040 (0.037, 112.310)	0.727		
HBsAg (positive)	1.939 (0.200, 18.795)	0.568		
HBeAg (positive)	1.094 (0.092, 12.960)	0.943		
Cirrhosis	0.315 (0.061, 1.617)	0.166		
High blood pressure	1.115 (0.284, 4.376)	0.876		
Diabetes mellitus	4.800 (0.404, 57.025)	0.214		
BCLC stage				
0	–	–		
A	0.364 (0.061, 2.185)	0.269		
B	0.600 (0.090, 3.986)	0.597		
C	Reference			
ALBI grade				
I	Reference			
II	0.592 (0.109, 3.227)	0.544		
III	2.071 (0.121, 35.605)	0.616		
Inflammation grade				
G1	–	–		
G2	0.307 (0.088, 1.073)	0.064		
G3	Reference			
LS value (kPa)	1.631 (1.066, 2.496)	0.024*	2.055 (1.238, 3.410)	0.005*

*, referred to P<0.05. PHRR, parenchymal hepatic resection rate; BMI, body mass index; ALB, albumin; ALT, alanine aminotransferase; AST, aspartate aminotransferase; ALP, alkaline phosphatase; GGT, γ-glutamyl transferase; TP, total protein; TBIL, total bilirubin; DBIL, direct bilirubin; HGB, hemoglobin; PLT, platelet count; PT, prothrombin time; INR, international normalized ratio; HBsAg, hepatitis B surface antigen; HBeAg, hepatitis B e antigen; BCLC, Barcelona Clinic Liver Cancer; ALBI, albumin-bilirubin; LS, liver stiffness; OR, odds ratio; CI, confidence interval.

By combining the two points above, we only included the PHRR of the three parameters for multivariable analysis. Our study also found that ALB was a liver regeneration-related factor in univariate analysis. ALB is primarily synthesized by hepatocytes (43), and the development of liver fibrosis (with reduced liver regeneration capacity) changes the hepatocellular function (44,45), which can lead to decreased ALB synthesis and low circulating ALB levels.

Subgroup analysis showed LS values correlated with RI only when PHRR was 30–50%, explicitly, in the intermediate PHRR group. As discussed above, as PHRR increases, the subsequent increase in cytokine concentration and blood flow ratio, as well as the relatively greater space for regeneration, could all promote regeneration of the remnant liver. When PHRR reaches relatively large values, the effect of factors involving the liver itself, such as the degree of liver fibrosis, on liver regeneration might be relatively reduced. A previous study (21) revealed that only PHRR, but not LS values, was a statistically significant factor influencing the liver RI. In addition, when PHRR is relatively small and the volume of remnant liver postoperatively is large, the liver volume needed to restore total liver volume is small, which limits the ability of the remnant liver to regenerate regardless of the degree of liver fibrosis. Therefore, the current data demonstrated that 30–50% was an appropriate range for PHRR in assessing the impact of liver fibrosis on regeneration, although additional studies are required to confirm this conclusion.

We also found that liver fibrosis stage and LS values of MRE were both associated with the presence of PLF. Liver fibrosis is the result of most kinds of chronic liver damage and is related to the potential development of liver failure (46,47). As stated above, LS values measured at MRE can be used to identify the grade of liver fibrosis and may be an independent factor of PLF.

There were several limitations to this study, including those inherent to a retrospective observational study design. First, the LS measurements in some patients may be affected by parenchymal inflammation, such as concomitant chronic viral hepatitis, but the effect may not be significant (17). In our study, while not statistically significant (r=0.128; P=0.355), the LS values of MRE showed a positive tendency with inflammation grade in all patients, although studies on chronic viral hepatitis have suggested inflammation does not influence the correlation between LS values and fibrosis staging (48,49). Another potential confounder of LS measurements is hepatic steatosis. We evaluated this by measuring the hepatic attenuation minus splenic attenuation difference on nonenhanced CT (50) and found it did not afflict any of the patients in our study. Thus, we did not include hepatic steatosis as a confounding factor when exploring the relationship between LS value and liver regeneration. Second, we performed histological analysis of liver parenchyma from resected specimens, and the results of fibrosis grading were used as the gold standard for assessing its extent in the entire remnant liver parenchyma after hepatectomy, which may overestimate the degree of fibrosis of the entire actual remnant liver. Therefore, in theory, we should have evaluated the extent of fibrosis in the entire remnant liver parenchyma. However, due to the nature of retrospective analysis, it was impractical to proceed with liver biopsy of the remnant liver parenchyma, and we only evaluated fibrosis in the liver parenchyma of the resected specimens. Third, owing to the retrospective design, the postoperative CT follow-up interval was not maintained consistently in all patients. However, previous studies (51,52) have demonstrated that the first postoperative week is quantitatively critical during the liver regeneration process, and subsequent regeneration increases at a slower pace. Therefore, while the time interval in our study was within an acceptable range, additional prospective studies are required to standardize the follow-up interval to improve the results.

In conclusion, LS values based on MRE exhibited reliable accuracy for the diagnosis of high RI. This noninvasive and quantitative imaging technique may be a useful preoperative predictor of liver regeneration for patients with PH.

Acknowledgments

Funding: This work was supported by the Science and Technology Support Program of Sichuan Province (Nos. 2021YFS0144, 2021YFS0021, and 2020YFS0121), China Postdoctoral Science Foundation (No. 2021M692289), and Post-Doctor Research Project, West China Hospital, Sichuan University (No. 2020HXBH130).

Footnote

Reporting Checklist: The authors have completed the STARD reporting checklist. Available at https://qims.amegroups.com/article/view/10.21037/qims-22-306/rc

Conflicts of Interest: All authors have completed the ICMJE uniform disclosure form (available at https://qims.amegroups.com/article/view/10.21037/qims-22-

306/coif). All authors report that this work was supported by the Science and Technology Support Program of Sichuan Province (No. 2021YFS0144, 2021YFS0021, and 2020YFS0121), China Postdoctoral Science Foundation (No. 2021M692289), and Post-Doctor Research Project, West China Hospital, Sichuan University (No. 2020HXBH130). LN and XW are employees of GE Healthcare. The authors have no other conflicts of interest to declare.

Ethical Statement: The authors are accountable for all aspects of the work in ensuring that questions related to the accuracy or integrity of any part of the work are appropriately investigated and resolved. The study was conducted in accordance with the Declaration of Helsinki (as revised in 2013). This retrospective study was approved by the institutional review board of the West China Hospital of Sichuan University, and individual consent for this retrospective analysis was waived.

References

1. Shi L, Liu B, Shen DD, Yan P, Zhang Y, Tian Y, Hou L, Jiang G, Zhu Y, Liang Y, Liang X, Shen B, Yu H, Zhang Y, Wang Y, Guo X, Cai X. A tumor-suppressive circular RNA mediates uncanonical integrin degradation by the proteasome in liver cancer. Sci Adv 2021;7:eabe5043.
2. Kudo M. Recent Advances in Systemic Therapy for Hepatocellular Carcinoma in an Aging Society: 2020 Update. Liver Cancer 2020;9:640-62.
3. Hayashi T, Shibata M, Oe S, Miyagawa K, Honma Y, Harada M. Antiplatelet Therapy Improves the Prognosis of Patients with Hepatocellular Carcinoma. Cancers (Basel) 2020;12:3215.
4. Wei L, Lee D, Law CT, Zhang MS, Shen J, Chin DW, Zhang A, Tsang FH, Wong CL, Ng IO, Wong CC, Wong CM. Genome-wide CRISPR/Cas9 library screening identified PHGDH as a critical driver for Sorafenib resistance in HCC. Nat Commun 2019;10:4681.
5. Xia Y, Li J, Liu G, Wang K, Qian G, Lu Z, Yang T, Yan Z, Lei Z, Si A, Wan X, Zhang H, Gao C, Cheng Z, Pawlik TM, Wang H, Lau WY, Wu M, Shen F. Long-term Effects of Repeat Hepatectomy vs Percutaneous Radiofrequency Ablation Among Patients With Recurrent Hepatocellular Carcinoma: A Randomized Clinical Trial. JAMA Oncol 2020;6:255-63.
6. Shimada M, Matsumata T, Maeda T, Itasaka H, Suehiro T, Sugimachi K. Hepatic regeneration following right lobectomy: estimation of regenerative capacity. Surg Today 1994;24:44-8.
7. Zappa M, Dondero F, Sibert A, Vullierme MP, Belghiti J, Vilgrain V. Liver regeneration at day 7 after right hepatectomy: global and segmental volumetric analysis by using CT. Radiology 2009;252:426-32.
8. Jiao LR, Fajardo Puerta AB, Gall TMH, Sodergren MH, Frampton AE, Pencavel T, Nagendran M, Habib NA, Darzi A, Pai M, Thomas R, Tait P. Rapid Induction of Liver Regeneration for Major Hepatectomy (REBIRTH): A Randomized Controlled Trial of Portal Vein Embolisation versus ALPPS Assisted with Radiofrequency. Cancers (Basel) 2019;11:302.
9. Golse N, Bucur PO, Adam R, Castaing D, Sa Cunha A, Vibert E. New paradigms in post-hepatectomy liver failure. J Gastrointest Surg 2013;17:593-605.
10. Qiu T, Fu R, Ling W, Li J, Song J, Wu Z, Shi Y, Zhou Y, Luo Y. Comparison between preoperative two-dimensional shear wave elastography and indocyanine green clearance test for prediction of post-hepatectomy liver failure. Quant Imaging Med Surg 2021;11:1692-700.
11. Haberman DM, Andriani OC, Segaran NL, Volpacchio MM, Micheli ML, Russi RH, Pérez Fernández IA. Role of CT in Two-Stage Liver Surgery. Radiographics 2022;42:106-24.
12. Ribero D, Amisano M, Bertuzzo F, Langella S, Lo Tesoriere R, Ferrero A, Regge D, Capussotti L. Measured versus estimated total liver volume to preoperatively assess the adequacy of the future liver remnant: which method should we use? Ann Surg 2013;258:801-6; discussion 806-7.
13. Uxa S, Castillo-Binder P, Kohler R, Stangner K, Müller GA, Engeland K. Ki-67 gene expression. Cell Death Differ 2021;28:3357-70.
14. Sheng RF, Yang L, Jin KP, Wang HQ, Liu H, Ji Y, Fu CX, Zeng MS. Assessment of liver regeneration after associating liver partition and portal vein ligation for staged hepatectomy: a comparative study with portal vein ligation. HPB (Oxford) 2018;20:305-12.

15. Park CC, Nguyen P, Hernandez C, Bettencourt R, Ramirez K, Fortney L, Hooker J, Sy E, Savides MT, Alquiraish MH, Valasek MA, Rizo E, Richards L, Brenner D, Sirlin CB, Loomba R. Magnetic Resonance Elastography vs Transient Elastography in Detection of Fibrosis and Noninvasive Measurement of Steatosis in Patients With Biopsy-Proven Nonalcoholic Fatty Liver Disease. Gastroenterology 2017;152:598-607.e2.
16. Kamada Y, Morishita K, Koseki M, Nishida M, Asuka T, Naito Y, Yamada M, Takamatsu S, Sakata Y, Takehara T, Miyoshi E. Serum Mac-2 Binding Protein Levels Associate with Metabolic Parameters and Predict Liver Fibrosis Progression in Subjects with Fatty Liver Disease: A 7-Year Longitudinal Study. Nutrients 2020;12:1770.
17. Hoodeshenas S, Yin M, Venkatesh SK. Magnetic Resonance Elastography of Liver: Current Update. Top Magn Reson Imaging 2018;27:319-33.
18. Wang XP, Wang Y, Ma H, Wang H, Yang DW, Zhao XY, Jin EH, Yang ZH. Assessment of liver fibrosis with liver and spleen magnetic resonance elastography, serum markers in chronic liver disease. Quant Imaging Med Surg 2020;10:1208-22.
19. Ouyang GX, Zhang YM, Zhu SL, Wang P, Ren Y, Li JH, Liu YK, Chen J, Xiang BD, Li LQ, Liu JY, Zhang ZM. A novel, non-invasive model for diagnosing liver fibrosis stage in patients with hepatocellular carcinoma. Sci Rep 2018;8:13074.
20. Abulkhir A, Limongelli P, Healey AJ, Damrah O, Tait P, Jackson J, Habib N, Jiao LR. Preoperative portal vein embolization for major liver resection: a meta-analysis. Ann Surg 2008;247:49-57.
21. Jang S, Lee JM, Lee DH, Joo I, Yoon JH, Chang W, Han JK. Value of MR elastography for the preoperative estimation of liver regeneration capacity in patients with hepatocellular carcinoma. J Magn Reson Imaging 2017;45:1627-36.
22. Kele PG, de Boer M, van der Jagt EJ, Lisman T, Porte RJ. Early hepatic regeneration index and completeness of regeneration at 6 months after partial hepatectomy. Br J Surg 2012;99:1113-9.
23. Park J, Kim JH, Kim JE, Park SJ, Yi NJ, Han JK. Prediction of liver regeneration in recipients after living-donor liver transplantation in using preoperative CT texture analysis and clinical features. Abdom Radiol (NY) 2020;45:3763-74.
24. Kim JE, Kim JH, Park SJ, Choi SY, Yi NJ, Han JK. Prediction of liver remnant regeneration after living donor liver transplantation using preoperative CT texture analysis. Abdom Radiol (NY) 2019;44:1785-94.
25. Nadalin S, Testa G, Malagó M, Beste M, Frilling A, Schroeder T, Jochum C, Gerken G, Broelsch CE. Volumetric and functional recovery of the liver after right hepatectomy for living donation. Liver Transpl 2004;10:1024-9.
26. Yokoi H, Isaji S, Yamagiwa K, Tabata M, Sakurai H, Usui M, Mizuno S, Uemoto S. Donor outcome and liver regeneration after right-lobe graft donation. Transpl Int 2005;18:915-22.
27. Bedossa P, Poynard T. An algorithm for the grading of activity in chronic hepatitis C. The METAVIR Cooperative Study Group. Hepatology 1996;24:289-93.
28. Ren H, Liu Y, Lu J, An W, Wang W, Yan T, Li Y, Dong J, Cai J. Evaluating the clinical value of MRI multi-model diffusion-weighted imaging on liver fibrosis in chronic hepatitis B patients. Abdom Radiol (NY) 2021;46:1552-61.
29. Rahbari NN, Garden OJ, Padbury R, Brooke-Smith M, Crawford M, Adam R, et al. Posthepatectomy liver failure: a definition and grading by the International Study Group of Liver Surgery (ISGLS). Surgery 2011;149:713-24.
30. Koo TK, Li MY. A Guideline of Selecting and Reporting Intraclass Correlation Coefficients for Reliability Research. J Chiropr Med 2016;15:155-63.
31. Inoue Y, Fujii K, Ishii M, Kagota S, Tomioka A, Hamamoto H, Osumi W, Tsuchimoto Y, Masubuchi S, Yamamoto M, Asai A, Komeda K, Shimizu T, Asakuma M, Fukunishi S, Hirokawa F, Narumi Y, Higuchi K, Uchiyama K. Volumetric and Functional Regeneration of Remnant Liver after Hepatectomy. J Gastrointest Surg 2019;23:914-21.
32. Venkatesh SK, Wang G, Lim SG, Wee A. Magnetic resonance elastography for the detection and staging of liver fibrosis in chronic hepatitis B. Eur Radiol 2014;24:70-8.
33. Tan CH, Venkatesh SK. Magnetic Resonance Elastography and Other Magnetic Resonance Imaging Techniques in Chronic Liver Disease: Current Status and Future Directions. Gut Liver 2016;10:672-86.
34. Idilman IS, Li J, Yin M, Venkatesh SK. MR elastography of liver: current status and future perspectives. Abdom Radiol (NY) 2020;45:3444-62.
35. Zheng Z, Wang B. The Gut-Liver Axis in Health and Disease: The Role of Gut Microbiota-Derived Signals in Liver Injury and Regeneration. Front Immunol 2021;12:775526.
36. Garcea G, Maddern GJ. Liver failure after major hepatic resection. J Hepatobiliary Pancreat Surg 2009;16:145-55.
37. Wiemann SU, Satyanarayana A, Tsahuridu M, Tillmann HL, Zender L, Klempnauer J, Flemming P, Franco

S, Blasco MA, Manns MP, Rudolph KL. Hepatocyte telomere shortening and senescence are general markers of human liver cirrhosis. FASEB J 2002;16:935-42.
38. Hemann MT, Strong MA, Hao LY, Greider CW. The shortest telomere, not average telomere length, is critical for cell viability and chromosome stability. Cell 2001;107:67-77.
39. Zou Y, Sfeir A, Gryaznov SM, Shay JW, Wright WE. Does a sentinel or a subset of short telomeres determine replicative senescence? Mol Biol Cell 2004;15:3709-18.
40. Ding BS, Cao Z, Lis R, Nolan DJ, Guo P, Simons M, Penfold ME, Shido K, Rabbany SY, Rafii S. Divergent angiocrine signals from vascular niche balance liver regeneration and fibrosis. Nature 2014;505:97-102.
41. Gruttadauria S, Parikh V, Pagano D, Tuzzolino F, Cintorino D, Miraglia R, Spada M, Vizzini G, Luca A, Gridelli B. Early regeneration of the remnant liver volume after right hepatectomy for living donation: a multiple regression analysis. Liver Transpl 2012;18:907-13.
42. Abdalla EK, Denys A, Chevalier P, Nemr RA, Vauthey JN. Total and segmental liver volume variations: implications for liver surgery. Surgery 2004;135:404-10.
43. Jagdish RK, Maras JS, Sarin SK. Albumin in Advanced Liver Diseases: The Good and Bad of a Drug! Hepatology 2021;74:2848-62.
44. Lee YA, Wallace MC, Friedman SL. Pathobiology of liver fibrosis: a translational success story. Gut 2015;64:830-41.
45. Bernardi M, Angeli P, Claria J, Moreau R, Gines P, Jalan R, Caraceni P, Fernandez J, Gerbes AL, O'Brien AJ, Trebicka J, Thevenot T, Arroyo V. Albumin in decompensated cirrhosis: new concepts and perspectives. Gut 2020;69:1127-38.
46. Jiao J, Friedman SL, Aloman C. Hepatic fibrosis. Curr Opin Gastroenterol 2009;25:223-9.
47. Campana L, Iredale JP. Regression of Liver Fibrosis. Semin Liver Dis 2017;37:1-10.
48. Crespo S, Bridges M, Nakhleh R, McPhail A, Pungpapong S, Keaveny AP. Non-invasive assessment of liver fibrosis using magnetic resonance elastography in liver transplant recipients with hepatitis C. Clin Transplant 2013;27:652-8.
49. Venkatesh SK, Xu S, Tai D, Yu H, Wee A. Correlation of MR elastography with morphometric quantification of liver fibrosis (Fibro-C-Index) in chronic hepatitis B. Magn Reson Med 2014;72:1123-9.
50. Park YS, Park SH, Lee SS, Kim DY, Shin YM, Lee W, Lee SG, Yu ES. Biopsy-proven nonsteatotic liver in adults: estimation of reference range for difference in attenuation between the liver and the spleen at nonenhanced CT. Radiology 2011;258:760-6.
51. Gong WF, Zhong JH, Lu Z, Zhang QM, Zhang ZY, Chen CZ, Liu X, Ma L, Zhang ZM, Xiang BD, Li LQ. Evaluation of liver regeneration and post-hepatectomy liver failure after hemihepatectomy in patients with hepatocellular carcinoma. Biosci Rep 2019;39:BSR20190088.
52. Haga J, Shimazu M, Wakabayashi G, Tanabe M, Kawachi S, Fuchimoto Y, Hoshino K, Morikawa Y, Kitajima M, Kitagawa Y. Liver regeneration in donors and adult recipients after living donor liver transplantation. Liver Transpl 2008;14:1718-24.

Cite this article as: Zhang T, Li Q, Wei Y, Yao S, Yuan Y, Deng L, Wu D, Nie L, Wei X, Tang H, Song B. Preoperative evaluation of liver regeneration following hepatectomy in hepatocellular carcinoma using magnetic resonance elastography. Quant Imaging Med Surg 2022;12(12):5433-5451. doi: 10.21037/qims-22-306

Supplementary

Table S1 MR imaging parameters

Sequence	Repetition time (ms)	Echo time (ms)	Field of view (cm^2)	Scan matrix	Slice thickness (mm)	Slice gap (mm)	Number of excitation
2D-flow-compensated GRE	1,000	65.6	42×42	80×80	8	2	1
In/out of phase T1WI	150	1.3/2.5	40×40	288×192	6	2	1
T2WI	2× RC	80	40×40	320×320	6	2	1.5
LAVA	6.0	1.4/2.7	38×30.4	300×256	4	0	1

MR, magnetic resonance; 2D, two-dimensional; GRE, gradient recalled echo; T1WI, T1-weighted imaging; T2WI, T2-weighted imaging; LAVA, liver acceleration volume acquisition; RC, respiratory cycle.

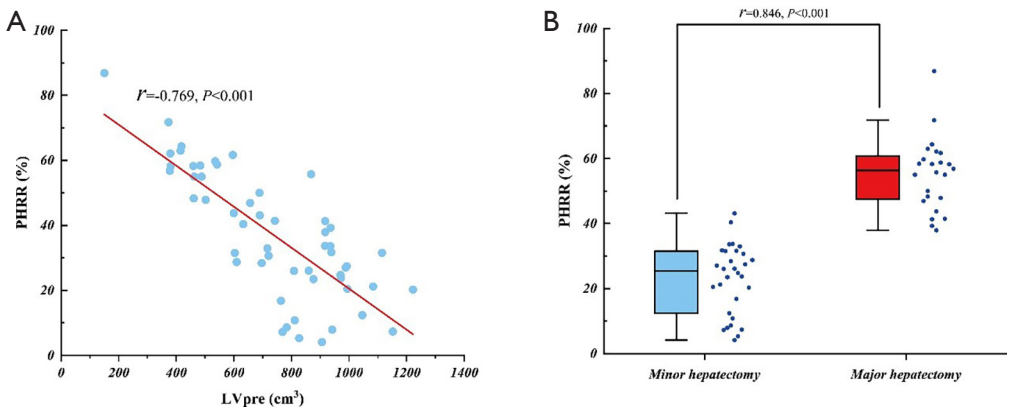

Figure S1 The relation between PHRR and LVpre (A), PHRR and the type of hepatectomy (B). PHRR, parenchymal hepatic resection rate; LVpre, volume of preoperative future liver remnant.

https://dx.doi.org/10.21037/qims-22-306

Table S2 Comparison of clinicopathologic characteristics of patients with low PHRR, intermediate PHRR and high PHRR

Clinicopathologic characteristics	Low PHRR (<30%, n=21)	Intermediate PHRR (30–50%, n=17)	High PHRR (>50%, n=16)	P value
RI				<0.001*
Low	21 (100.00)	10 (58.82)	2 (82.50)	
High	0 (0.00)	7 (41.18)	14 (87.50)	
RI (%)	18.65±10.48	39.78±23.75	96.66±57.96	<0.001*
Age (years)	51.52±11.91	52.76±9.82	49.88±11.40	0.499
Gender				0.406
Male	17 (80.95)	16 (94.12)	13 (81.25)	
Female	4 (19.05)	1 (5.88)	3 (18.75)	
PHRR (%)	18.01±8.70	38.59±6.16	61.00±8.43	<0.001*
LVpre (cm^3)	908.15±151.11	764.57±182.80	476.03±157.79	<0.001*
LVpost (cm^3)	1,052.42±168.00	1,028.40±169.75	962.27±207.62	0.320
BMI (kg/m^2)	22.66±3.58	24.08±3.69	23.17±2.64	0.641
Tumor size (cm)	4.22±2.07	6.23±4.27	7.54±3.87	0.017*
Multifocality	6 (28.57)	5 (29.42)	6 (37.50)	0.825
ALB (g/L)	39.92±5.38	41.74±5.91	43.53±4.80	0.139
ALT (IU/L)	77.71±152.60	113.71±310.31	102.00±250.27	0.485
AST (IU/L)	102.00±250.27	138.88±433.95	110.81±202.82	0.909
ALP (IU/L)	92.29±34.67	105.35±57.09	106.31±30.70	0.209
GGT (IU/L)	87.14±83.54	113.82.85.36	109.88±62.05	0.368
AST/ALT	1.09±0.33	1.09±0.38	1.03±0.44	0.616
TP (g/L)	67.63±9.53	68.91±6.39	69.63±9.59	0.633
TBIL (μmol/L)	16.24±7.54	12.00±3.70	14.37±6.01	0.420
DBIL (μmol/l)	5.92±4.40	4.32±2.23	5.36±2.87	0.66
HGB (g/L)	141.52±23.76	138.94±21.68	142.69±19.50	0.874
PLT (10^9/L)	138.09±71.18	156.00±88.99	172.50±66.97	0.144
PT (s)	12.71±3.93	12.63±4.39	13.15±5.31	0.773
INR	1.04±0.19	1.02±0.09	1.06±0.12	0.815
HBsAg (positive)	19 (90.48)	16 (94.12)	14 (87.50)	0.793
HBeAg (positive)	2 (9.52)	1 (5.88)	0 (0.00)	0.223
Anti-HCV (positive)	0 (0.00)	1 (5.88)	0 (0.00)	0.910
Cirrhosis	16 (76.19)	13 (76.47)	12 (75.00)	0.938
Ascites	0 (0.00)	0 (0.00)	1 (6.25)	0.184
High blood pressure	6 (28.57)	2 (11.76)	4 (25.00)	0.726
Diabetes mellitus	0 (0.00)	1 (5.88)	2 (12.50)	0.103
BCLC stage				0.116
0	1 (4.76)	1 (5.88)	0 (0.00)	

Table S2 *(continued)*

https://dx.doi.org/10.21037/qims-22-306

Table S2 *(continued)*

Clinicopathologic characteristics	Low PHRR (<30%, n=21)	Intermediate PHRR (30–50%, n=17)	High PHRR (>50%, n=16)	P value
A	14 (66.67)	10 (58.82)	6 (37.50)	
B	4 (19.05)	6 (35.29)	6 (37.50)	
C	2 (0.52)	0 (0.00)	4 (25.00)	
ALBI grade				0.248
I	14 (66.67)	14 (82.35)	15 (93.75)	
II	6 (28.57)	2 (11.76)	1 (6.25)	
III	1 (4.76)	1 (5.88)	0 (0.00)	
Type of hepatectomy				<0.001*
Minor (<3 Couinaud segments)	21 (100.00)	9 (52.94)	0 (0.00)	
Major (≥3 Couinaud segments)	0 (0.00)	8 (45.06)	16 (100.00)	
Inflammation grade				0.992
G1	2 (9.52)	0 (0.00)	2 (12.50)	
G2	9 (42.86)	9 (52.94)	6 (37.50)	
G3	10 (47.62)	8 (47.06)	8 (50.00)	
Fibrosis stage				0.599
F0–1	2 (9.52)	4 (23.53)	4 (25.00)	
F2–3	13 (61.91)	7 (41.18)	7 (43.75)	
F4	6 (28.57)	6 (35.29)	5 (31.25)	
LS value (kPa)	4.65±1.05	4.30±1.79	3.72±1.61	0.183

Data are represented in mean ± SD or n (%). Data were evaluated by variance analysis or Wilcoxon rank-sum test for continuous variables and the chi-square test or Fisher's exact test or Wilcoxon rank-sum test for categorical variables. *, referred to P<0.05. PHRR, parenchymal hepatic resection rate; RI, regeneration index; LVpre, volume of preoperative future liver remnant; LVpost, volume of postoperative liver remnant; BMI, body mass index; ALB, albumin; ALT, alanine aminotransferase; AST, aspartate aminotransferase; ALP, alkaline phosphatase; GGT, γ-glutamyl transferase; TP, total protein; TBIL, total bilirubin; DBIL, direct bilirubin; HGB, hemoglobin; PLT, platelet count; PT, prothrombin time; INR, international normalized ratio; HBsAg, hepatitis B surface antigen; HBeAg, hepatitis B e antigen; anti-HCV, hepatitis C virus antibody; BCLC, Barcelona Clinic Liver Cancer; ALBI, albumin-bilirubin; LS, liver stiffness.

https://dx.doi.org/10.21037/qims-22-306

Table S3 Results of the univariate analysis of correlations between the RI and clinical-imaging characteristic

Baseline characteristics	Low PHRR (<30%, n=21)		Intermediate PHRR (30–50%, n=17)		High PHRR (>50%, n=16)	
	Correlation coefficient	P value	Correlation coefficient	P value	Correlation coefficient	P value
Age (years)	0.109	0.639	0.106	0.686	–0.162	0.549
PHRR (%)	0.077	0.741	0.412	0.101	0.391	0.134
BMI (kg/m^2)	–0.055	0.814	–0.191	0.462	0.197	0.464
Tumor size (cm)	–0.270	0.236	–0.052	0.844	–0.469	0.067
Multifocality	0.157	0.498	0.237	0.359	0.420	0.105
ALT (IU/L)	–0.174	0.451	0.193	0.459	0.159	0.557
AST (IU/L)	–0.081	0.728	–0.012	0.963	0.122	0.652
ALP (IU/L)	0.062	0.790	0.406	0.106	–0.137	0.613
GGT (IU/L)	–0.029	0.900	0.248	0.338	–0.483	0.058
AST/ALT	0.04	0.865	–0.197	0.448	0.046	0.867
TP (g/L)	0.108	0.640	–0.069	0.793	0.288	0.279
ALB (g/L)	–0.216	0.348	0.378	0.135	0.374	0.154
TBIL (μmol/L)	–0.196	0.393	0.204	0.433	–0.078	0.774
DBIL (μmol/l)	0.096	0.678	0.037	0.892	–0.122	0.652
HGB (g/L)	0.146	0.527	0.238	0.358	–0.212	0.431
PLT (10^9/L)	–0.073	0.754	0.301	0.240	–0.05	0.854
PT (s)	–0.101	0.663	–0.080	0.761	0.046	0.866
INR	–0.073	0.752	–0.275	0.285	0.063	0.815
HBsAg (positive)	–0.107	0.644	0.408	0.104	–0.123	0.650
HBeAg (positive)	–0.402	0.071	–0.306	0.232	–	–
Anti-HCV (positive)	–	–	–0.153	0.557	–	–
Cirrhosis	–0.148	0.523	–0.170	0.515	0.501	0.205
Ascites	–	–	–	–	–0.084	0.757
High blood pressure	–0.331	0.143	-0.037	0.887	–0.063	0.818
Diabetes mellitus	–	–	0.204	0.432	0.041	0.880
BCLC stage	–0.149	0.518	–0.192	0.461	–0.354	0.179
ALBI grade	0.249	0.276	–0.282	0.273	–0.435	0.092
LS value	–0.034	0.884	–0.799	<0.001*	–0.244	0.362

*, referred to P<0.05. RI, regeneration index; PHRR, parenchymal hepatic resection rate; BMI, body mass index; ALT, alanine aminotransferase; AST, aspartate aminotransferase; ALP, alkaline phosphatase; GGT, γ-glutamyl transferase; TP, total protein; ALB, albumin; TBIL, total bilirubin; DBIL, direct bilirubin; HGB, hemoglobin; PLT, platelet count; PT, prothrombin time; INR, international normalized ratio; HBsAg, hepatitis B surface antigen; HBeAg, hepatitis B e antigen; anti-HCV, hepatitis C virus antibody; BCLC, Barcelona Clinic Liver Cancer; ALBI, albumin-bilirubin; LS, liver stiffness.

https://dx.doi.org/10.21037/qims-22-306

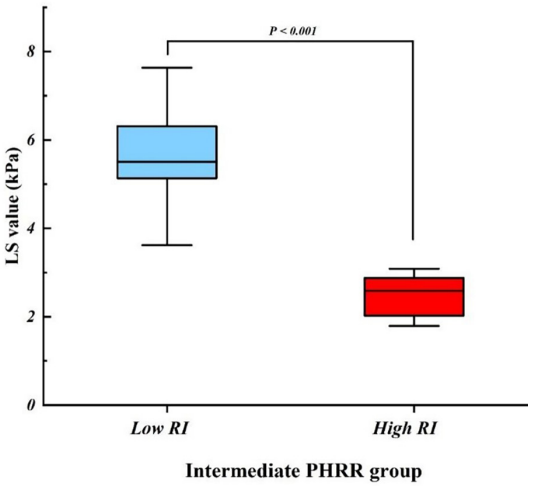

Figure S2 Comparison of LS values between the intermediate PHRR subgroup with high RI and low RI. LS, liver stiffness; RI, regeneration index; PHRR, parenchymal hepatic resection rate.

Table S4 Comparison of baseline characteristics of patients with low RI and high RI in intermediate PHRR group

Baseline characteristics	Low RI (n=10)	High RI (n=7)	P value
Age (years)	51.20±10.33	55.00±9.35	0.364
Gender			1.000
Male	9 (90.00)	7 (100.00)	
Female	1 (10.00)	0 (0.00)	
RI (%)	24.42±13.52	61.72±16.59	<0.001*
PHRR (%)	36.56±4.32	41.50±7.52	0.193
LVpre (cm^3)	871.33±145.93	612.07±105.04	0.005*
LVpost (cm^3)	1,069.50±170.55	969.69±162.38	0.230
BMI (kg/m^2)	24.91±3.87	22.89±3.32	0.315
Tumor size (cm)	6.60±5.08	5.61±3.03	0.635
Multifocality	2 (20.00)	3 (42.86)	0.309
ALT (IU/L)	158.40±406.58	49.86±26.97	0.193
AST (IU/L)	212.10±565.84	34.29±14.81	0.813
ALP (IU/L)	97.80±70.98	116.14±30.06	0.070
GGT (IU/L)	91.60±66.93	145.57±103.49	0.315
AST/ALT	1.19±0.31	0.94±0.44	0.133
TP (g/L)	68.90±7.57	68.93±4.79	0.813
ALB (g/L)	39.69±6.21	44.66±4.27	0.070
TBIL (μmol/L)	11.36±4.14	12.91±3.01	0.270
DBIL (μmol/l)	4.74±2.89	4.13±0.93	0.918
HGB (g/L)	136.90±24.84	141.86±17.62	0.536

Table S4 *(continued)*

https://dx.doi.org/10.21037/qims-22-306

Table S4 *(continued)*

Baseline characteristics	Low RI (n=10)	High RI (n=7)	P value
PLT (10^9/L)	132.00±67.30	190.29±109.50	0.230
PT (s)	13.52±5.63	11.36±0.84	0.475
INR	1.04±0.10	0.99±0.04	0.364
HBsAg (positive)	9 (90.00)	7 (100.00)	0.388
HBeAg (positive)	1 (10.00)	0 (0.00)	0.388
Anti-HCV (positive)	1 (10.00)	0 (0.00)	0.388
Cirrhosis	8 (80.00)	5 (71.43)	0.682
High blood pressure	1 (10.00)	1 (14.28)	1.000
Diabetes mellitus	0 (0.00)	1 (14.28)	0.412
BCLC stage			0.375
0	0 (0.00)	1 (14.29)	
A	6 (60.00)	4 (57.14)	
B	4 (40.00)	2 (28.57)	
C	0 (0.00)	0 (0.00)	
ALBI grade			0.565
I	8 (80.00)	6 (85.71)	
II	1 (10.00)	1 (14.29)	
III	1 (10.00)	0 (0.00)	
Type of hepatectomy			0.153
Minor (<3 Couinaud segments)	7 (70.00)	2 (28.57)	
Major (≥3 Couinaud segments)	3 (30.00)	5 (71.43)	
Inflammation grade			1.000
G1	0 (0.00)	0 (0.00)	
G2	5 (50.00)	4 (57.14)	
G3	5 (50.00)	3 (42.86)	
Fibrosis stage			0.001*
F0–1	0 (0.00)	4 (51.14)	
F2–3	4 (40.00)	3 (42.86)	
F4	6 (60.00)	0 (0.00)	
LS value (kPa)	5.56±1.15	2.51±0.46	<0.001*

Data are represented in mean ± SD or n (%). And Data were evaluated by independent *t*-test or Mann-Whitney U test for continuous variables and the chi-square test or Fisher's exact test for categorical variables. *, referred to P<0.05. RI, regeneration index; PHRR, parenchymal hepatic resection rate; LVpre, volume of preoperative future liver remnant; LVpost, volume of postoperative liver remnant; BMI, body mass index; ALT, alanine aminotransferase; AST, aspartate aminotransferase; ALP, alkaline phosphatase; GGT, γ-glutamyl transferase; TP, total protein; ALB, albumin; TBIL, total bilirubin; DBIL, direct bilirubin; HGB, hemoglobin; PLT, platelet count; PT, prothrombin time; INR, international normalized ratio; HBsAg, hepatitis B surface antigen; HBeAg, hepatitis B e antigen; anti-HCV, hepatitis C virus antibody; BCLC, Barcelona Clinic Liver Cancer; ALBI, albumin-bilirubin; LS, liver stiffness.

https://dx.doi.org/10.21037/qims-22-306

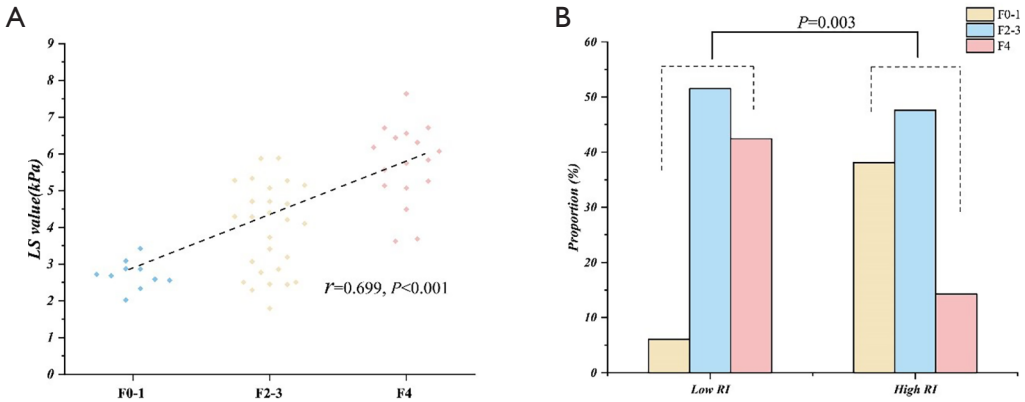

Figure S3 LS values between patients with different fibrosis stage (A), and comparison of fibrosis stage between patients with high RI and low RI (B). LS, liver stiffness; RI, regeneration index.

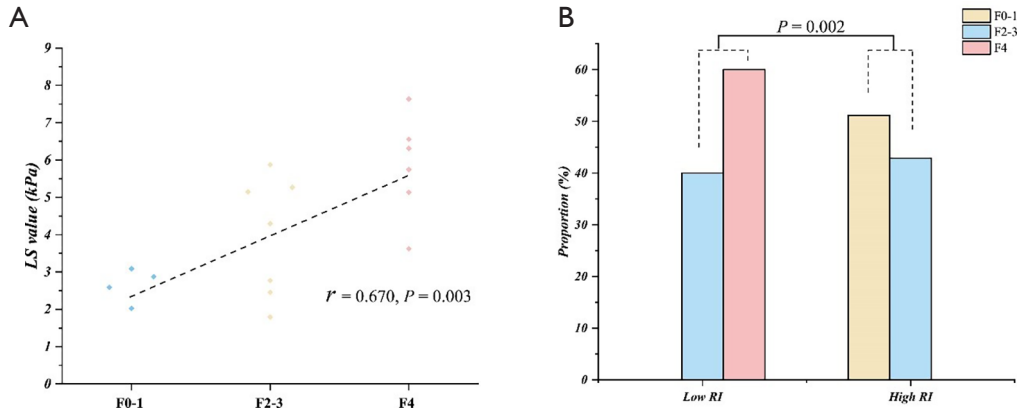

Figure S4 LS values between patients with different fibrosis stage (A) and comparison of fibrosis stage between patients with high RI and low RI (B) in intermediate PHRR subgroup. LS, liver stiffness; RI, regeneration index; PHRR, parenchymal hepatic resection rate.

https://dx.doi.org/10.21037/qims-22-306